JURNAL ILMU LINGKUNGAN
Volume 24 Issue 1 (2026) : 136-146 *ISSN 1829-8907*

Assessing Urban Heat Island Impact on Environmental Criticality Index in Padang City, Indonesia

Yulia Fitri Harahap[1*], Fitra Armando[1], Edo Nofriadi[1], and Intan Lestari Mulyaning Tyas[2]

[1]Department of Environmental Science, Faculty of Mathematics and Natural Science, Universitas Negeri Padang, Indonesia; e-mail: yuliafitrihrp@unp.ac.id
[2]Department of Natural Science Education, Faculty of Mathematics and Natural Science, Universitas Negeri Padang, Indonesia

ABSTRAK

Urbanisasi yang pesat dan hilangnya vegetasi secara signifikan memperparah fenomena Urban Heat Island (UHI), yang berdampak pada meningkatnya kerentanan ekologis di kota-kota pesisir tropis. Penelitian ini mengevaluasi hubungan spasial antara pemanasan kota dan degradasi lingkungan di Kota Padang, Indonesia—sebuah kota pesisir tropis berukuran sedang yang dicirikan oleh pembangunan pesat dan transisi topografi yang tajam dari dataran rendah pantai ke pegunungan di sisi timur. Menggunakan citra satelit Landsat 8 (Januari 2023–Januari 2024) yang diproses melalui Google Earth Engine (GEE), penelitian ini mengintegrasikan Land Surface Temperature (LST), Normalized Difference Vegetation Index (NDVI), dan indeks lahan terbangun untuk memetakan intensitas UHI dan Environmental Criticality Index (ECI). Hasil penelitian menunjukkan dikotomi lingkungan barat-timur yang kontras: dataran rendah pesisir barat yang padat bangunan bertindak sebagai pusat akumulasi panas (titik panas perkotaan), menunjukkan nilai NDVI rendah (mencapai -0,35), nilai LST maksimum sebesar 33,47°C, dan tingkat kekritisan lingkungan yang tinggi (mencakup 6,92% dari total luas wilayah). Sebaliknya, zona pegunungan di bagian timur secara alami memitigasi stres termal karena tutupan kanopi hutan yang tinggi dan keuntungan laju penurunan suhu lingkungan berdasarkan ketinggian (environmental lapse rate). Analisis statistik mengonfirmasi adanya korelasi positif yang kuat antara ECI dan LST (r=0,72) membuktikan bahwa pemanasan suhu permukaan kota secara langsung memicu degradasi lingkungan yang lebih luas. Meskipun dibatasi oleh penggunaan data observasi satu tahun dan kurangnya validasi lapangan secara langsung, penelitian ini memberikan kerangka kerja baru dalam memetakan kerentanan ekologis. Temuan ini menekankan urgensi kebijakan tata ruang yang tangguh iklim di Kota Padang, termasuk kewajiban penerapan infrastruktur hijau-biru skala bangunan (green roofs dan green walls) di pusat kota barat yang padat, serta pengetatan kuota ruang terbuka hijau (RTH) minimal 30% di zona sub-urban yang sedang berkembang.

Keywords: *Urban Heat Island, Environmental Criticality Index, Land Surface Temperature,* Penginderaan Jauh, *Google Earth Engine*, Kota Padang

ABSTRACT

Rapid urbanization and vegetation loss significantly intensify the Urban Heat Island (UHI) effect, escalating ecological vulnerability in tropical coastal cities. This study evaluates the spatial relationship between urban warming and environmental degradation in Padang City, Indonesia—a medium-sized tropical coastal city characterized by rapid development and a sharp topographic transition from coastal lowlands to eastern mountains. Utilizing Landsat 8 satellite imagery (January 2023–January 2024) processed via Google Earth Engine (GEE), this research integrates Land Surface Temperature (LST), Normalized Difference Vegetation Index (NDVI), and built-up indices to map UHI intensity and the Environmental Criticality Index (ECI). The results reveal a stark west-east environmental dichotomy: the highly built-up western coastal lowlands act as intensive urban heat hotspots, exhibiting low NDVI values (down to -0.35), maximum LST values of 33.47°C, and high environmental criticality (covering 6.92% of the total area). Conversely, the eastern mountainous zone naturally mitigates thermal stress due to high forest canopy cover and environmental lapse rate benefits. Statistical analysis confirms a strong positive correlation between ECI and LST (r=0.72), demonstrating that urban overheating directly drives broader environmental degradation. Although limited by a single-year dataset and a lack of in-situ validation, this study provides a novel framework for mapping ecological vulnerability. These findings underscore the urgent need for climate-resilient spatial planning in Padang, including mandatory building-scale blue-green infrastructure (green roofs and walls) in the dense western core and strict enforcement of a minimum 30% green open space (RTH) quota in expanding sub-urban zones.

***Keywords*:** Urban Heat Island, Environmental Criticality Index, Land Surface Temperature, Remote Sensing, Google Earth Engine, Padang City

Citation: Harahap, Y. F., Armando, F., Nofriadi, E., and Tyas, I. L. M. (2026). Assessing Urban Heat Island Impact on Environmental Criticality Index in Padang City, Indonesia. Jurnal Ilmu Lingkungan, 24(1), 136-146, doi:10.14710/jil.24.1.136-146

1. INTRODUCTION

Urban heat island (UHI) refers to the phenomenon where urban areas experience higher temperatures than rural areas (Xiang et al., 2024). Research consistently indicates a strong correlation between Land Use and Land Cover (LULC) changes and Land Surface Temperature (LST), with highly built-up areas exhibiting pronounced thermal disparities compared to suburban regions (Coseo & Larsen, 2014; Irshad et al., 2024; Kafy et al., 2021). This phenomenon is caused by the acceleration of population growth and rapid urbanization that leads to an increase in the demand for residential and commercial spaces. The process involves replacing natural vegetation with impervious poses with low water permeability with hardened surfaces in urban areas, leading to restriction of water infiltration and evaporation in the hydrological cycle, thereby diminishing the natural cooling effect (Fattah et al., 2021). The low albedo of building surfaces leads to increased heat absorption, combined with a low heat capacity, which contributes to the intensification of the UHI phenomenon. This highlights the urgent need for integrated urban planning strategies that address LULC dynamics to mitigate UHI impacts and foster sustainable, cooler urban environments.

The UHI phenomenon impacts both human and nature due to exacerbating temperature changes in urban areas. Moreover, the UHI effect increases individual vulnerability to heat-related illnesses, which can potentially lead to higher mortality rates (Santamouris, 2018). The negative impact of the UHI effect on human health and the environment has drawn significant attention from researchers and stakeholders. It is crucial to study the factors influencing the UHI effect, as well as to explore strategies for improving the urban thermal environment and mitigating its effects in urban areas. The Environmental Criticality Index (ECI) is one of the environmental indices based on temperature and vegetation cover. ECI can be used to find out the areas that were the most critically affected by the UHI phenomenon. The study indicates a close relationship between ECI and LST; ECI is directly proportional to LST, while it is inversely related to vegetation cover (Darmawan & Barry, 2022).

The exacerbation of the UHI issues significantly affects human health and urban ecosystems. It significantly heightens individual susceptibility to heat-related illnesses, perhaps resulting in increased mortality rates (Santamouris, 2020a). Driven by the urgent need to mitigate these adverse socio-environmental effects, researchers have developed spatial assessment tools such as the Environmental Criticality Index (ECI). Based on the integration of surface temperature and vegetation density, the ECI serves as an effective metric to identify zones most critically affected by urban thermal stress. Empirical evidence indicates that the ECI is directly proportional to Land Surface Temperature (LST) and inversely proportional to vegetation cover (Darmawan & Barry, 2022), making it a robust proxy for mapping urban environmental vulnerability.

Monitoring air temperature by deploying instruments at various locations throughout the city is one of the methods used to study the UHI effect. However, this approach cannot represent the overall UHI effect in the city due to a limited number of points that are unevenly distributed. While numerical modeling can overcome this limitation by generating geographically continuous data (Kolokotroni et al., 2012), these techniques are computationally complex, particularly when predicting energy exchange processes within intricate metropolitan structures (Zhou et al., 2019). To address these challenges, the application of Geographic Information Systems (GIS) coupled with satellite remote sensing has emerged as a powerful approach. Satellite imagery offers extensive spatial coverage, long-term historical archives, and high-resolution data, providing consistent and reproducible Earth observations that enable the examination of urban thermal environments across local to global and daily to interannual scales (Deilami et al., 2018).

Padang is the capital city of West Sumatera, characterized by high population growth of 1.26% per year in 2024, leading to intensive land-use change from vegetation cover area to hardened surface area and exacerbating the increase of temperature in this area. In addition to rapid expansion, Padang possesses unique geographical and environmental characteristics that increase its vulnerability to environmental degradation. The city is situated in a tropical coastal area characterized by elevated humidity, intense sun radiation, and intricate topography between coastal lowlands and adjacent hills. These circumstances render Padang particularly susceptible to temperature stress, ecological strain, and climate-related threats. The growing prevalence of developed land alongside diminishing green spaces may intensify environmental challenges and diminish urban ecological resilience (Sidiqui et al., 2022).

Previously, the UHI studies in Indonesia and tropical cities were mainly focused on land surface temperature, distribution, urban thermal comfort, vegetation change, or heat-related hazards separately. Land Surface Temperature (LST) and Universal Thermal Climate Index (UTCI) have been used to study heat stress distribution and UHI health concerns in Padang City previously (Driptufany & Fajrin, 2021; Pertiwi et al., 2024; Sari, 2020). However, there is a lack of studies that integrate analysis to evaluate the relationship between urban thermal conditions and environmental degradation simultaneously in Padang City. In other tropical coastal cities like Denpasar, Indonesia, and Matara, Sri Lanka, UHI indicators and ECI or Temperature Criticality Value (TCV) were found to improve environmental vulnerability assessment in rapidly urbanizing areas (Gede et al., 2023; Jayasinghe et al., 2024). Integrated approaches are constrained, particularly in medium-sized tropical coastal cities. Prior research has concentrated on

thermal characteristics or socio-economic susceptibility without correlating biophysical heat intensity to environmental significance. Consequently, a spatially integrated UHI–ECI framework for medium-sized tropical coastal towns such as Padang, characterized by rapid urban growth, coastal climatic conditions, and diminishing green spaces that may heighten environmental sensitivity, is absent. This study addresses this gap by integrating Urban Heat Island analysis and Environmental Criticality Index assessment using satellite imagery and GIS techniques to evaluate the spatial relationship between urban warming and environmental degradation in Padang City. The study contributes to the limited body of research focusing on medium-sized tropical coastal cities and provides spatial information that can support climate-resilient urban planning and sustainable land management.

2. METHODOLOGY

2.1. Data Collection and Processing

This study was conducted using Landsat 8 Collection 2 Tier 1 Top of Atmosphere (TOA) imagery accessed and processed through Google Earth Engine (GEE) with Path 128 and Row 058. The image acquisition ranged from the 1st of January 2023 to the 1st of January 2024. Landsat satellite imagery data is utilized in this research because its thermal infrared sensors allow for an in-depth analysis of land surface temperature. All images covering the study area were composited utilizing the median composite approach to mitigate temporal noise and enhance image stability.

To improve the accuracy of vegetation indices and LST calculation due to cloud cover in the study area, cloud masking was applied to eliminate cloud and cloud-shadow pixels that could interfere with spectral reflectance and thermal information extraction. Cloud masking was executed utilizing the QA_PIXEL quality assessment band present in Landsat 8 Collection 2 data. Pixels classified as cloud and cloud shadow were eliminated via a bitwise masking technique. Bit 5 was designated for identifying cloud pixels, whereas bit 3 was allocated for identifying cloud shadow pixels. Only pixels devoid of cloud cover were preserved for further investigation.

2.2. Estimation of LST using Landsat Data

LST is calculated using data from the thermal bands, which provide valuable insights into the temperature variations of the Earth's surface (bands 4, 5, and 10) of Landsat data using the GEE platform for the year 2023. Calculation of LST involved obtaining Normalized Difference Vegetation Index (NDVI), proportion of vegetation (Pv), land surface emissivity, and brightness temperature (Xiang et al., 2024).

2.2.1. Calculation of NDVI

Land greenness is quantified by NDVI using the satellite infrared (IR) and near infrared (NIR) bands (Abdullah et al., 2022). NDVI values range between -1 and 1; the closer the NDVI to -1, the lower the vegetation cover of the pixel is, and vice versa.

NDVI is calculated following this equation:

$$INDVI = \frac{(NIR - RED)}{(NIR + RED)}$$

For Landsat 8:

$$aNDVI = \frac{(Band\ 5 - Band\ 4)}{(Band\ 5 + Band\ 5)}$$

where;
NIR = near-infrared band value
RED = infrared band value

2.2.2. Proportion of Vegetation (Pv)

PV is the area under vegetation cover compared to the total area percentage. The calculation of the PV is shown in the equation below:

$$Pv = (\frac{NDVI - NDVImin}{NDVImax + NDVImin})^2$$

NDVI min refers to the value of NDVI in an area that is covered by bare land or uncovered by vegetation, while NDVI max refers to the value of NDVI in an area that is completely covered by vegetation.

2.2.3. Emissivity of Land Surface (E)

Emissivity of land surface is the ratio emitted by objects in relation to the heating land. Land surface emissivity is calculated following the equation:

$$E = 0{,}004\ x\ Pv + 0{,}986$$

2.2.4. Sensor Brightness Temperature Estimation (BT)

Top of Atmosphere (TOA) is needed to calculate brightness temperature. The calculation using the following equation:

$$ToA = 0{,}0003343\ x\ Band\ 10 + 0{,}1$$

BT value calculated by:

$$BT\ (℃) = \left(\frac{1321{,}0789}{Ln\ \left(\frac{774{,}8853}{ToA}\right)}\right) - 273{,}15$$

2.2.5. Calculation of LST

LST is computed by NDVI, PV, E, and BT parameters. Next, it can be derived by applying the equation provided below:

$$LST = \frac{BT}{[1 + \left(0{,}00115\ x\ \frac{BT}{1{,}4388}\right) x\ In\ (E)]}$$

2.3. UHI Intensity Classification

UHI intensity is calculated using normalized LST data following the equation:

$$Ni = \frac{(Ti + Tmin)}{(Tmax + Tmin)}$$

Where:
Ni = normalized value of UHI
Ti = LST absolute temperature of the image element.
Tmin = minimum value of LST
Tmax = maximum value of LST
And the larger value of Ni indicates the higher value of the UHI effect in the study area.

In this research, the mean-standard deviation method is utilized to examine and assess the spatial patterns of the UHI effect that are categorized into five classes (Table 1).

Table 1. Classification of UHI Class

Class	*Ni* range
Low	*Ni* < mean–1.5 sd
Sub-Low	Nmean–1.5sd < Ni < Nmean-0.5sd
Middle	Nmean-0.5sd<*Ni*<Nmean+0.5sd
Sub-High	Nmean + 0.5sd < Ni < Nmean + 1.5sd
High	*Ni*>Nmean+1.5sd

Nmean = normalized LST mean
sd = normalized LST standard deviation

2.4. Calculation of ECI

2.4.1. Modified Normalized Difference Built-up Index (MNDBI)

MNDBI is known as the most effective transformation algorithm for built-up area identification. NDBI and ECI are closely correlated; the higher the NDBI value, the higher the ECI. The equation of NDBI is shown in the equation below:

$$MNDBI = \frac{(SWIR + NIR)}{(SWIR + NIR)}$$

For Landsat 8:

$$MNDBI = \frac{(Band\ 7 - Band\ 5)}{(Band\ 7 + Band\ 5)}$$

SWIR = shortwave-infrared band value

2.4.2. Normalized Difference Water Index (NDWI)

NDWI is utilized as an extraction of a water body. The water body and cloud must be the exception to the critical land category. The NDWI values range between -1 and 1. The equation of NDWI is shown in the equation below:

$$NDWI = \frac{(GREEN + SWIR)}{(GREEN + SWIR)}$$

For Landsat 8:

$$NDWI = \frac{(Band\ 3 - Band\ 6)}{(Band\ 3 + Band\ 6)}$$

GREEN = green band value
SWIR = shortwave-infrared band value.

2.4.3. Environmental Critically Index (ECI)

In this study, ECI value is calculated by modifying the equation developed by Senanayake et al. (2013) with added NDBI and NDBI values. To avoid the number 0 of the pixel, it is done by stretching the pixel value's range between 1 and 255. The NDVI is calculated following the equation below:

$$ECI\ (streched) = \frac{(LST * MNDBI\ (streched)}{(NDVI * NDWI\ (streched)}$$

The result of ECI calculation followed by the classification using the histogram equalization method into three classes of the ECI. These classes are high, middle, and low critic. The total area is calculated by multiplying the total cells for each class by 900 m^2 (Landsat spatial resolution is 30 m).

3. RESULT AND DISCUSSION

3.1. Analysis of NDVI and LST

NDVI spatial distribution in Padang City is displayed in Figure 1. The range value of NDVI is between -0.35 and 0.83. The high NDVI value area is 80.47% of the total area, while the low NDVI area is 19.52% of the total area. Higher NDVI values indicate more vegetation cover in the area. The areas with high vegetation cover in Padang City are concentrated in the east part of the city. These areas are mainly covered by forest in mountainous areas and farmland such as rice fields and dry fields. Lower values of NDVI mostly concentrate in urban areas with low vegetation cover due to intensive built-up processes. On the other hand, the lowest value of NDVI, -0.3, is concentrated in the west part of the city. These areas are poorly green spaces with dense buildings. The characteristic of the area correlates with NDVI, which is impacted by the total vegetation cover.

Figure 2 shows the estimation of the LST result of Padang City that ranges between 8°C and 33°C. It means dominant in high-temperature zones located in the west of the city, while it decreases to the east.

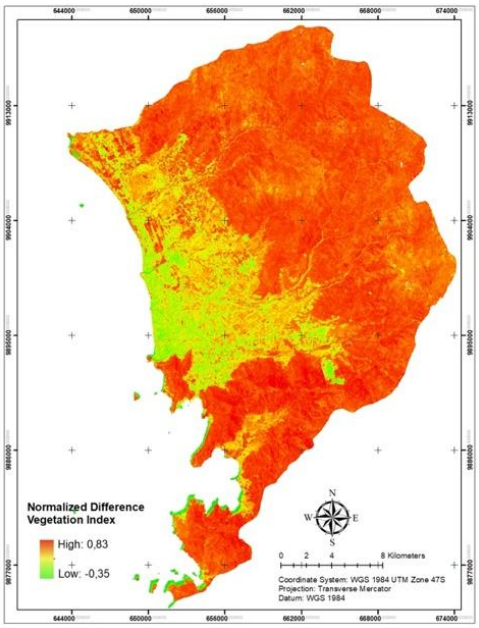

Figure 1. Distribution of NDVI

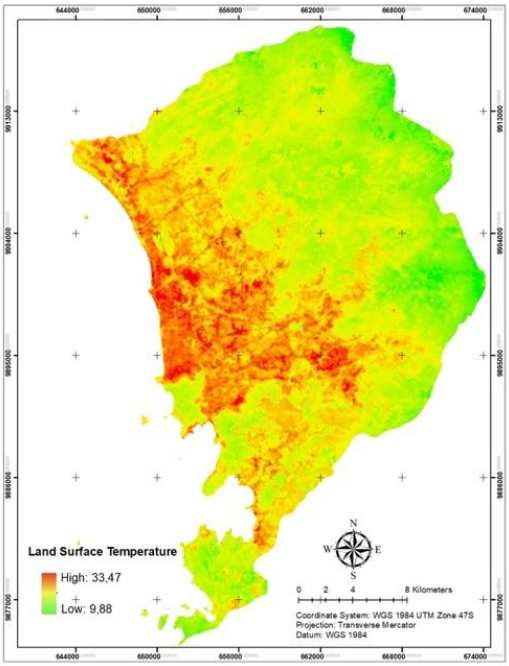

Figure 2. Distribution of LST

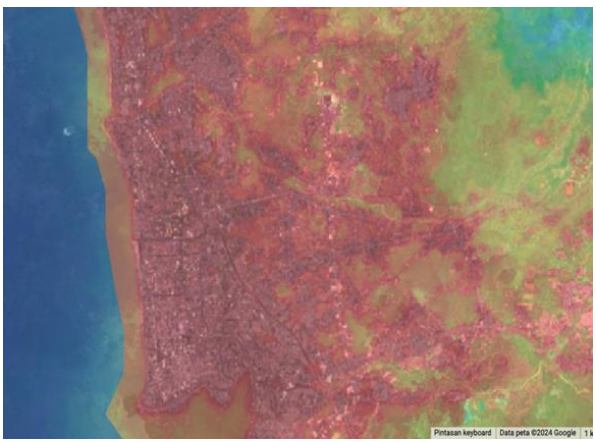

Figure 3. High LST in Urban Area

High-temperature areas are mainly distributed in urban areas with a high density of buildings on the west. The west part of Padang City is the main concentration of urban buildings, with the center of government office activities, trading areas, and universities, resulting in high temperatures due to high heat absorption of building materials. Urban environments are relatively warm due to the natural surface energy and radiation balances being altered by these urban characteristics. Changes in the urban heat canopy layer happen near the surface of cities and reach about the average height of buildings (Kabano et al., 2021). Urban heat islands are a result of these changes, which have also an impact on the environment's thermal, radiative, moisture, and aerodynamic properties. As a result, a significant portion of the vegetative cover in cities has been replaced by built-up surfaces, which at night absorb and reradiate solar light. The urban canopy layer refers to the section of the planetary boundary layer that is directly impacted by the presence of urban environments. This layer is shaped primarily by local or micro-scale processes specific to the urban area. It is characterized by the interaction between the urban surface and atmospheric conditions. These localized influences play a crucial role in determining the unique climatic characteristics of urban areas, distinguishing them from surrounding rural or natural environments (Weng et al., 2004).

In contrast, low-temperature areas in the east of the city are mainly characterized by covered vegetation such as forest and farmland. The areas found near rivers and reservoirs are have low temperatures too. In addition to providing shade, vegetation plays a crucial role in enhancing air humidity and cooling the surrounding environment by absorbing heat through the process of water evaporation. It not only raises humidity levels but also helps to mitigate the urban heat island effect. By releasing moisture into the air, vegetation reduces the amount of solar radiation absorbed by the ground and buildings, leading to a decrease in their surface temperatures. As a result, the air temperature around these areas is also lowered, contributing to a more comfortable and cooler microclimate in urban settings.

Water in the study area has the lowest NDVI and LST values. The aforementioned explanation is because the underlying surface's ability to store heat through structural change and transpiration evaporation is what primarily drove the vegetation's influence on surface radiation temperature. The absence of vegetation on the urban surface contributes to its high calorific capacity, as the dry, non-evapotranspiration character of the constituent material results in a high pad surface thermal conductivity. However, in shallow marsh, the amount of sensible heat and also latent heat that can be retained in a surface water column is limited, which causes the surface temperature to rise quickly. During the day, excess heat energy gained from solar

radiation is released, raising the wetland water body temperature surface and raising the surrounding ground and air (Jia et al., 2020).

Research indicates there is clear evidence that NDVI negatively correlates with LST (Ahmad et al., 2024). Rise in temperature amplifies the cooling impact of vegetation, strengthening the negative link between LST and NDVI. Amount of vegetation cover biomass has lower levels of CO_2 leading to the increasing of the heating process, as indicated by the negative association between NDVI and LST. Due to the significant correlation between those, if NDVI measurements for the research area are available, there is a greater chance that LST may be predicted from direct relapse (Hussain & Karuppannan, 2023).

3.2. UHI Effect in Padang City

The UHI effect was categorized by normalizing the LST data. The calculation revealed that the mean of the normalized LST (Ni) is 0.50, with a standard deviation of 0.30. Table 2 details the spatial distribution of the UHI intensity classes in Padang City.

Table 2. UHI Distribution Class

Class	*Ni* Range	Area (Ha)	Area (%)
Low	Ni<0.03	3.33	0.01
Sub Low	0.03 < Ni < 0.3	494.01	0.72
Middle	0.3 < Ni < 0.6	49068.9	71.72
Sub-High	0.6 < Ni < 0.96	18823.68	27.51
High	Ni > 0.96	27	0.04

Table 2 reveals that the majority of Padang City is in the medium class of the UHI effect intensity with 71.72%. It can be seen that the sub-high area is 27.51% of the area of Padang City, the sub-low area is 0.72%, the high area is 0.04%, and the low area is 0.02%. The distribution of the LST in Figure 2 presents a consistent pattern with the distribution of the UHI provided in Table 2. The LST map shows several areas with high temperatures, yet the UHI categorization shows that most of the study area is middle class, and 27.51% is sub-high class. This shows that the UHI phenomena in the studied area are not confined to extreme hot places and have extended with moderate to high intensity. Conversely, the High class only accounts for 0.04% of the total region, indicating that the locations with extremely high UHI intensity are limited to select areas that serve as heat accumulation centers (urban hotspots). The heterogeneity of the UHI effect in Padang City is potentially influenced by a combination of land use, climatic, topographical, and human activity.

Spatial analysis indicates that the western region of Padang City experiences a higher UHI effect than the eastern region. The western urban zone is highly built-up, characterized by a high concentration of concrete, steel, and glass. These materials possess high thermal conductivity and rapidly absorb solar radiation. Consequently, surface temperatures elevate rapidly, a process further exacerbated by the high sensible heat flux that quickly absorbs and releases heat. Conversely, the eastern part of the city experiences a lower UHI effect due to extensive vegetation cover. Vegetation effectively mitigates surface temperatures through transpiration and shading processes.

The alterations in the thermal environment resulting from urbanization vary markedly between the urban (western) and rural (eastern) areas. The severity of the UHI effect is mostly influenced by these variables in Padang City. Initially, there are distinctions between urban and rural areas regarding the nature and intensity of human activity present in each. These disparities manifest in various forms, including population density, air quality, and additional factors, all of which ultimately influence temperature. Secondly, due to significant disparities between the foundational surfaces and atmospheric conditions of urban and rural territorial systems that influence temperature and induce changes in the intensity of the UHI, identical meteorological elements may exert divergent impacts on each (Liu & Masago, 2025).

Meteorological factors and human activity affect UHI, either enchanching or weaking (Zhang et al., 2023). The regional environmental system influenced by a number of climatic elements, including wind speed, relative humidity, atmospheric circulation, solar radiation, precipitation, and others, affects UHI intensity (Manoli et al., 2019). Furthermore, topographically, Padang City exhibits a stark contrast, transitioning from flat coastal lowlands in the west to mountainous terrain in the east. This complex topography significantly affects the UHI distribution, as higher elevations naturally experience lower temperatures due to the environmental lapse rate, while the flat lowlands trap heat and limit effective thermal dispersion.

3.3. Environment Critcal Index (ECI) in Padang City

ECI data in Padang City was obtained from NDVI, MNDWI, MNDBI and LST data. Figure 4 and Table 3 show the map of ECI spatial distribution and total class area in Padang City. NDVI and LST values are directly correlated with ECI. NDVI has negative correlation with ECI, while LST has positive correlation with ECI values. NDVI refer to total area vegetation cover, higher vegetation cover leading to lower environmentally critically class. Vegetation acts as a thermal insulator between the ground and t and affects the reducing temperature fluctuations and affects the height expansion of the Earth's boundary layer. It makes cloudiness and also surfaces radiation. These properties improve the quality of the environment. In difference, high value of LST exacerbates the criticality of the environment. Elevated city temperatures significantly elevate detrimental pollutants' density, such as particulate matter and ground-level ozone (Lai & Cheng, 2009)

There is ample evidence linking urban overheating to ground-level ozone, and the primary factor raising ozone concentrations above recommended levels appears to be urban heat islands.

Table 3. ECI Class Distribution

ECI Class	Area (Ha)	Area (%)
Low	26,872.38	39.29
Middle	36797.58	53.80
High	4732.74	6.92

It can be shown that approximately a half of the total area in Padang City experienced a middle critical index. The middle class of ECI are mostly in the center to the east of the area in Padang City. These areas are characterized by a low density of buildings and high vegetation cover. On the other hand, high critical class is concentrated in the west part of the city by 6.92% of the total area. It can be concluded that the west part of the city has the worst environmental quality, while the center and the east have better environmental quality.

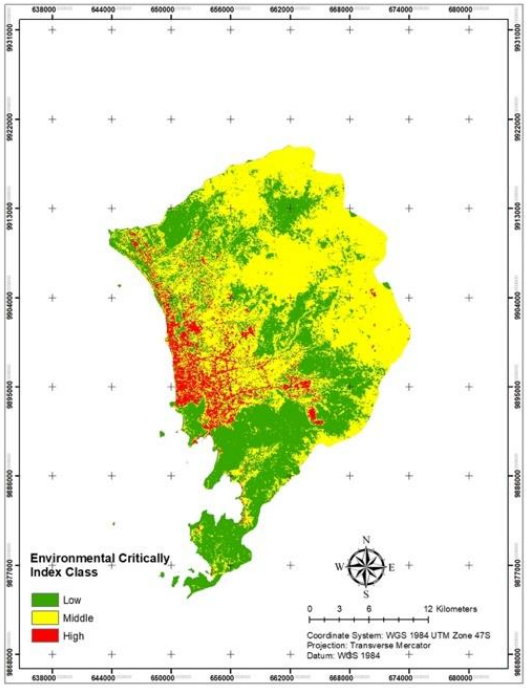

Figure 4. Distribution of ECI Class

The high ECI class in the west part of Padang city is impacted by urban activity, causing a higher temperature in this area. Furthermore, high temperature exacerbates environmental quality, increasing air pollution by promoting the development of ozone and particle pollution. Urban activity elevated urban ambient temperatures significantly, affecting the citizens and environmental life quality. Urban overheating has been shown to have a number of negative effects, including increased peak electricity demand, energy consumption for cooling, local vulnerability, heat-related mortality and morbidity, and also dangerous pollutant concentrations (Santamouris, 2015).

3.4. Distribution of ECI classes over UHI intensity

Linear statistical analysis was calculated to investigate the relationship between UHI effect distribution and ECI. The LST values was used to represent the UHI effect (Figure 5).

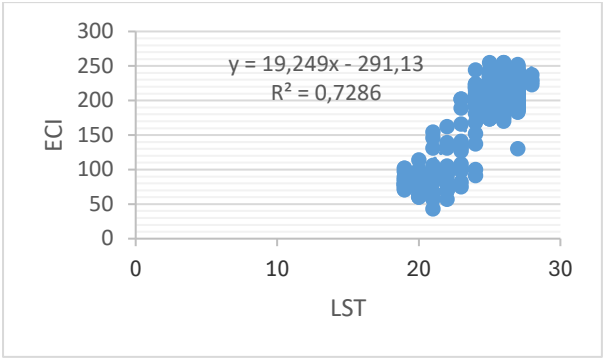

Figure 5. Correlation of ECI and UHI

Pearson correlation analysis revealed a strong positive relationship between ECI and LST (r = 0.72). This result indicates that areas characterized by higher land surface temperatures generally exhibit higher environmental criticality levels. The coefficient of determination (R^2 = 0.52) suggests that approximately 52% of the variability in ECI can be associated with variations in LST. However, the relationship should be interpreted as an association rather than direct causation, as other environmental and anthropogenic factors may also influence ECI.

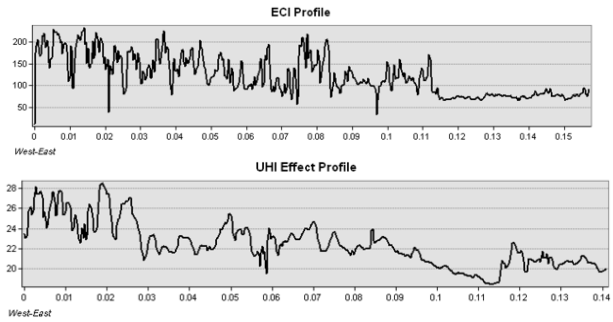

Figure 6. Transverse Profile of ECI and UHI

The relationship between ECI classes over UHI intensity in this study can be shown in Figure 7. The middle class of ECI, predominantly in this research, concentrated in the center and east area of Padang city. These areas experienced middle and sub-high UHI classes. The middle and sub-high classes of the UHI effect refer to 17 – 32°C temperatures. The majority middle class of ECI was impacted by middle-class UHI (17-28°C), distributed in the center of Padang City. These areas are characterized by a suburban area with a lower density of built-up area than the west part of the city but a higher densce build-up area than the east part.

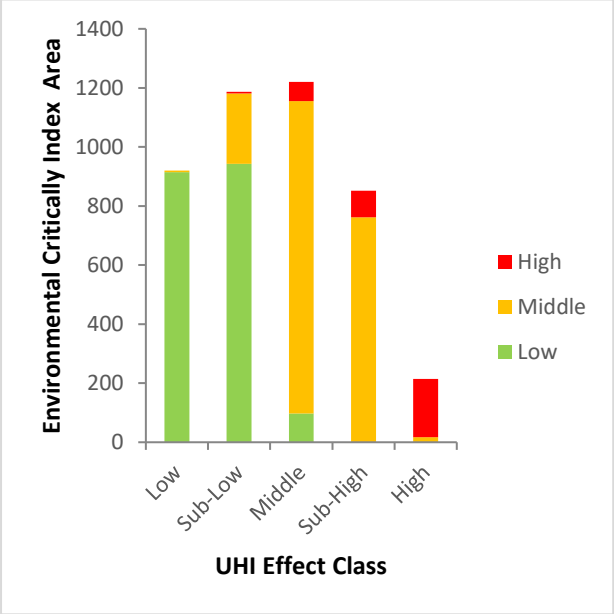

Figure 7. Distribution of ECI over UHI Class

Low environmental critical index in Padang City experienced low and sub-low UHI effects of 9–16°C temperatures, concentrated in the east of Padang City. The topography in these areas is mainly hilly and mountainous; these physical types of land surface impact microclimate in these areas. The temperature decreases with the increase of altitude. Consequently, the areas in the east of Padang city experienced cooler temperatures than the west part. Temperatures decrease as a result of the reduced heat retention capacity and thinner air at higher altitudes. This is influenced by the bulk of the atmosphere, air pressure, and air expansion. The air pressure is at its highest at sea level, which is why temperatures are frequently higher. The temperature decreases as one ascends due to the reduced air pressure. The probability of gas molecules colliding is diminished as the air expands as it ascends. This process is analogous to the expansion and cooling of air that is emitted from an automobile tire. The atmosphere becomes thinner as the altitude increases, as more heat is lost to space at higher altitudes, making it more challenging to maintain heat.The urban areas in the west of Padang City have the highest ECI and UHI effect. High ECI class predominantly located in high UHI intensity class, concentrate in the dense build-up area. Elevated urban ambient temperatures significantly affect the quality of the environment in general (Santamouris, 2020b). Urban overheating has been shown to have a number of negative effects, including increased peak electricity demand, energy consumption for cooling, local vulnerability, heat-related mortality and morbidity, and concentrations of dangerous pollutants.

NDVI, MNDWI and MNDBI that were used to quantify ECI can be used for analyzing the relationship between ECI and the UHI effect that is related to LST. NDVI and MNDWI have a negative correlation to LST. MNDWI indicated the cooling influence of water over the surrounding land surface temperature, which likewise exhibits a weak and negative correlation with LST. Increasing water temperature probability is caused by heat-absorbing substance contamination that is represented by the weak relationship of LST and MNDWI. MNDBI had a positive correlation to LST, indicating a considerable contribution from urban built-up land expansion to raising the LST (Roy et al., 2020). Additionally, NDBI-NDVI and NDBI-NDWI were investigated and were known to be negative in this research between MNDBI and NDVI and MNDWI. It can be concluded that higher values of NDBI and LST will raise the UHI effect and ECI, while NDVI and MNDWI lower the UHI effect and ECI in Padang city.

3.5. Spatial Planning and Mitigation Strategies

To mitigate the UHI effect in Padang City, intervention should be integrated between urban design, urban greening and blue-green infrastructure, and high-albedo surfaces and pavement. The expansion of green infrastructure in urban areas has been shown to be an effective method of mitigating Urban Heat Island (UHI) in numerous studies. Shade and evapotranspiration processes are facilitated by urban vegetation, which encompasses urban forests, street trees, green corridors, and parks, thereby diminishing air and surface temperatures. Previous research has indicated that green spaces can reduce the temperature of the adjacent area by approximately 1–5 °C, thereby enhancing the quality of the urban environment and thermal comfort (Cheela et al., 2021; Marando et al., 2022)

The implementation of green roofs and green walls has been acknowledged as an effective strategy for mitigating heat accumulation at the building scale. Green roofs have the potential to reduce the temperature of the roof surface and reduce the energy required to chill the building. Their efficacy is further improved by the implementation of suitable irrigation systems and the selection of vegetation that is tailored to the local climate (D. Li et al., 2014; Wang et al., 2022a; Wong et al., 2021)

The utilization of high-albedo surfaces, such as cool roofs and cool pavements, has been demonstrated to be effective in reducing the intensity of UHI by increasing solar reflectivity and minimizing heat absorption, in addition to greening strategies. These measures have the potential to reduce the energy consumption for ventilation and lower the ambient temperature. Consequently, the most effective method for achieving sustainable UHI mitigation in urban environments is the integration of green infrastructure, reflective surfaces, and supportive urban planning policies (Irfeey et al., 2023; Santamouris, 2014; Wang et al., 2022b).

4. CONCLUSION

The spatial dynamics of NDVI, LST, UHI intensity, and Environment Critical Index (ECI) have been synchronized in this study to map the ecological vulnerability of Padang City. The integrated

framework that integrates micro-climatic thermal stress (UHI) with comprehensive environmental degradation indices (ECI) is the structural novelty of this research. This framework captures the intricate influence of coastal-to-mountainous topography on urban thermodynamics. The empirical results indicate a significant environmental divide between the west and east. The densely populated western coastal lowlands are intensive heat accumulation areas (urban hotspots) with sub-high to high UHI classes and high environmental criticality (ECI) as a result of the lack of vegetation and the high density of concrete infrastructure. Furthermore, the mountainous and rural eastern region naturally reduces thermal stress by means of forest-driven evapotranspiration, higher altitudes, and moisture retention. Urban overheating serves as a direct cause of broader environmental degradation, including thermal distress and air quality hazards, as evidenced by the robust positive correlation between LST and ECI (r=0.72).

The limitation of this study primarily the absence of extensive in-situ field validation for surface temperature and air quality parameters, and the use of a one-year observation dataset that does not permit long-term temporal trajectories. Despite these insights, the study is not without its limitations.

In order to fill these voids, Padang City must transition from traditional zoning to spatial policies that are specifically designed to be climate-resilient. These policies can have practical implications for sustainable urban planning. In the critical western urban zone, where there are few large-scale parks, planning agencies should mandate the construction of blue-green infrastructure on a large scale. This should be primarily focused on the high-rise trading and government zone, where verdant roofs and walls, as well as high-albedo cool pavements, are required to modify surface radiation balances. Simultaneously, the spatial planning of the sub-urban central zone must establish strict green open space (RTH) quotas, with a minimum of 30% coverage, by incorporating green corridors and urban enclaves into the development of residential areas before the western core undergoes intensive built-up processes. The natural cooling mechanism and environmental lapse rate benefits of the eastern mountainous catchment must be preserved by legally safeguarding the ecological integrity from urban development. This will ensure the long-term microclimate stability of the entire city.

REFERENCES

Ahmad, B., Najar, M. B., & Ahmad, S. (2024). Analysis of LST, NDVI, and UHI patterns for urban climate using Landsat-9 satellite data in Delhi. *Journal of Atmospheric and Solar-Terrestrial Physics*, *265*, 106359. https://doi.org/10.1016/J.JASTP.2024.106359

Cheela, V., John, M., Biswas, W., & Sarker, P. (2021). Combating Urban Heat Island Effect—A Review of Reflective Pavements and Tree Shading Strategies. *Buildings*, *11*(3), 93. https://doi.org/10.3390/buildings11030093

Coseo, P., & Larsen, L. (2014). How factors of land use/land cover, building configuration, and adjacent heat sources and sinks explain Urban Heat Islands in Chicago. *Landscape and Urban Planning*, *125*, 117–129. https://doi.org/10.1016/J.LANDURBPLAN.2014.02.019

Darmawan[1], S., & Barry[2], A. L. (n.d.). Analisis Fenomena Urban Heat Island Menggunakan Google Earth Engine (Studi kasus: Jawa Barat, Indonesia). In *FTSP Series*. Retrieved http://tanahair.indonesia.go.id,

Deilami, K., Kamruzzaman, M., & Liu, Y. (2018). Urban heat island effect: A systematic review of spatio-temporal factors, data, methods, and mitigation measures. *International Journal of Applied Earth Observation and Geoinformation*, *67*, 30–42. https://doi.org/10.1016/J.JAG.2017.12.009

Driptufany, D., & Fajrin. (2021). Early detection of the distribution of heat stress hazards for sustainable land use planning In Padang City. *IOP Conference Series: Earth and Environmental Science*, *708*. https://doi.org/10.1088/1755-1315/708/1/012059

Fattah, M. A., Morshed, S. R., & Morshed, S. Y. (2021). Impacts of land use-based carbon emission pattern on surface temperature dynamics: Experience from the urban and suburban areas of Khulna, Bangladesh. *Remote Sensing Applications: Society and Environment*, *22*, 100508. https://doi.org/10.1016/J.RSASE.2021.100508

Gede, K., Putra, A., Risdiyanto, I., & Hidayat, R. (2023). Correlation Analysis Between Urban Heat Island Intensity and Temperature Criticality Value in Denpasar City. *Agromet*. https://doi.org/10.29244/j.agromet.37.2.66-76

Hussain, S., & Karuppannan, S. (2023). Land use/land cover changes and their impact on land surface temperature using remote sensing technique in district Khanewal, Punjab Pakistan. *Geology, Ecology, and Landscapes*, *7*(1), 46–58. https://doi.org/10.1080/24749508.2021.1923272

Irfeey, A. M. M., Chau, H.-W., Sumaiya, M. M. F., Wai, C. Y., Muttil, N., & Jamei, E. (2023). Sustainable Mitigation Strategies for Urban Heat Island Effects in Urban Areas. *Sustainability*, *15*(14), 10767. https://doi.org/10.3390/su151410767

Irshad, Z., Hassan, M., Akbar, S., Farooq, M., & Chishtie, F. A. (2024). Spatiotemporal changes in LULC and associated impact on urban Heat Islands over Pakistan using geospatial techniques. *Urban Climate*, *57*. https://doi.org/10.1016/j.uclim.2024.102112

Jayasinghe, C., Withanage, N., Mishra, P. K., Abdelrahman, K., & Fnais, M. (2024). Evaluating Urban Heat Islands Dynamics and Environmental Criticality in a Growing City of a Tropical Country Using Remote-Sensing Indices: The Example of Matara City, Sri Lanka. *Sustainability*. https://doi.org/10.3390/su162310635

Jia, Q., Zhou, L., Yu, W., Wang, X., Wen, R., & Xie, Y. (2020). Surface Energy Flux Changes and Budget in a Typical Coastal Reed Wetland (Liaohe Delta, China). *Journal of Coastal Research*, *36*(5), 1005–1012. https://doi.org/10.2112/JCOASTRES-D-19-00156.1

Kabano, P., Lindley, S., & Harris, A. (2021). Evidence of urban heat island impacts on the vegetation growing season length in a tropical city. *Landscape and Urban Planning*, *206*, 103989. https://doi.org/10.1016/J.LANDURBPLAN.2020.103989

Kafy, A. Al, Dey, N. N., Al Rakib, A., Rahaman, Z. A., Nasher, N. M. R., & Bhatt, A. (2021). Modeling the relationship between land use/land cover and land surface temperature in Dhaka, Bangladesh using CA-ANN algorithm. *Environmental Challenges*, *4*, 100190. https://doi.org/10.1016/J.ENVC.2021.100190

Kolokotroni, M., Ren, X., Davies, M., & Mavrogianni, A. (2012). London's urban heat island: Impact on current and future energy consumption in office buildings. *Energy and Buildings*, *47*, 302–311. https://doi.org/10.1016/J.ENBUILD.2011.12.019

Lai, L. W., & Cheng, W. L. (2009). Air quality influenced by urban heat island coupled with synoptic weather patterns. *Science of the Total Environment*, *407*(8), 2724–2733. https://doi.org/10.1016/j.scitotenv.2008.12.002

Li, D., Bou-Zeid, E., & Oppenheimer, M. (2014). The effectiveness of cool and green roofs as urban heat island mitigation strategies. *Environmental Research Letters*, *9*(5), 055002. https://doi.org/10.1088/1748-9326/9/5/055002

Li, L., Manier, H., & Manier, M. A. (2020). Integrated optimization model for hydrogen supply chain network design and hydrogen fueling station planning. *Computers & Chemical Engineering*, *134*, 106683. https://doi.org/10.1016/J.COMPCHEMENG.2019.106683

Liu, F., & Masago, Y. (2025). Assessing the geographical diversity of climate change risks in Japan by overlaying climatic impacts with exposure and vulnerability indicators. *Science of The Total Environment*, *959*, 178076. https://doi.org/10.1016/J.SCITOTENV.2024.178076

Manoli, G., Fatichi, S., Schläpfer, M., Yu, K., Crowther, T. W., Meili, N., Burlando, P., Katul, G. G., & Bou-Zeid, E. (2019). Magnitude of urban heat islands largely explained by climate and population. *Nature*, *573*(7772), 55–60. https://doi.org/10.1038/s41586-019-1512-9

Marando, F., Heris, M. P., Zulian, G., Udías, A., Mentaschi, L., Chrysoulakis, N., Parastatidis, D., & Maes, J. (2022). Urban heat island mitigation by green infrastructure in European Functional Urban Areas. *Sustainable Cities and Society*, *77*, 103564. https://doi.org/10.1016/j.scs.2021.103564

Pertiwi, M. D., Putri, S., Afifah, N., & Islamisari, W. (2024). Identification of Urban Heat Island (UHI) in the City of Padang from 2019-2023 using Multitemporal Images Case Study: Padang City Area, West Sumatra. *Sustainability (STPP) Theory, Practice and Policy*. https://doi.org/10.30631/sdgs.v4i1.2584

Roy, S., Pandit, S., Eva, E. A., Bagmar, M. S. H., Papia, M., Banik, L., Dube, T., Rahman, F., & Razi, M. A. (2020). Examining the nexus between land surface temperature and urban growth in Chattogram Metropolitan Area of Bangladesh using long term Landsat series data. *Urban Climate*, *32*, 100593. https://doi.org/10.1016/J.UCLIM.2020.100593

Santamouris, M. (2014). Cooling the cities – A review of reflective and green roof mitigation technologies to fight heat island and improve comfort in urban environments. *Solar Energy*, *103*, 682–703. https://doi.org/10.1016/j.solener.2012.07.003

Santamouris, M. (2015). Regulating the damaged thermostat of the cities - Status, impacts and mitigation challenges. In *Energy and Buildings* (Vol. 91, pp. 43–56). Elsevier Ltd. https://doi.org/10.1016/j.enbuild.2015.01.027

Santamouris, M. (2020a). Recent progress on urban overheating and heat island research. Integrated assessment of the energy, environmental, vulnerability and health impact. Synergies with the global climate change. *Energy and Buildings*, *207*, 109482. https://doi.org/10.1016/J.ENBUILD.2019.109482

Santamouris, M. (2020b). Recent progress on urban overheating and heat island research. Integrated assessment of the energy, environmental, vulnerability and health impact. Synergies with the global climate change. *Energy and Buildings*, *207*, 109482. https://doi.org/10.1016/J.ENBUILD.2019.109482

Sari, P. (2020). Assessing Health Risk For Community Adaptation In Urban Heat Island Area Of Padang City. *Jurnal Keselamatan Kesehatan Kerja Dan Lingkungan*. https://doi.org/10.25077/jk3l.1.1.12-26.2020

Senanayake, I. P., Welivitiya, W. D. D. P., & Nadeeka, P. M. (2013). Remote sensing based analysis of urban heat islands with vegetation cover in Colombo city, Sri Lanka using Landsat-7 ETM+ data. *Urban Climate*, *5*, 19–35. https://doi.org/10.1016/J.UCLIM.2013.07.004

Sidiqui, P., Roös, P. B., Herron, M., Jones, D. S., Duncan, E., Jalali, A., Allam, Z., Roberts, B. J., Schmidt, A., Tariq, M. A. U. R., Shah, A. A., Khan, N. A., & Irshad, M. (2022). Urban Heat Island vulnerability mapping using advanced GIS data and tools. *Journal of Earth System Science*, *131*(4), 266. https://doi.org/10.1007/s12040-022-02005-w

Wang, X., Li, H., & Sodoudi, S. (2022a). The effectiveness of cool and green roofs in mitigating urban heat island and improving human thermal comfort. *Building and Environment*, *217*, 109082. https://doi.org/10.1016/j.buildenv.2022.109082

Wang, X., Li, H., & Sodoudi, S. (2022b). The effectiveness of cool and green roofs in mitigating urban heat island and improving human thermal comfort. *Building and Environment*, *217*, 109082. https://doi.org/10.1016/j.buildenv.2022.109082

Weng, Q., Lu, D., & Schubring, J. (2004). Estimation of land surface temperature–vegetation abundance relationship for urban heat island studies. *Remote Sensing of Environment*, *89*(4), 467–483. https://doi.org/10.1016/J.RSE.2003.11.005

Wong, N. H., Tan, C. L., Kolokotsa, D. D., & Takebayashi, H. (2021). Greenery as a mitigation and adaptation strategy to urban heat. *Nature Reviews Earth & Environment*, *2*(3), 166–181. https://doi.org/10.1038/s43017-020-00129-5

Xiang, X., Zhai, Z., Fan, C., Ding, Y., Ye, L., & Li, J. (2024). Modelling future land use land cover changes and their impacts on urban heat island intensity in Guangzhou, China. *Journal of Environmental Management*, *366*. https://doi.org/10.1016/j.jenvman.2024.121787

Zhang, W., Li, Y., Zheng, C., & Zhu, Y. (2023). Surface urban heat island effect and its driving factors for all the

cities in China: Based on a new batch processing method. *Ecological Indicators*, *146*, 109818. https://doi.org/10.1016/J.ECOLIND.2022.109818

Zhou, D., Xiao, J., Bonafoni, S., Berger, C., Deilami, K., Zhou, Y., Frolking, S., Yao, R., Qiao, Z., & Sobrino, J. A. (2019). Satellite remote sensing of surface urban heat islands: Progress, challenges, and perspectives. In *Remote Sensing* (Vol. 11, Number 1). MDPI AG. https://doi.org/10.3390/rs11010048